Sustainable bio-oil from banana peel waste biomass: Optimization study and effect of thermal drying

Huang Shen Chua[1,2,5], Muhammad Faris Shah Bin Shabuddin[3], Kiat Moon Lee[4], Tan Kok Tat[1], Mohammed JK Bashir[1]*

[1]Faculty of Engineering and Green Technology (FEGT), Universiti Tunku Abdul Rahman, 31900 Kampar, Perak, Malaysia.
[2]Department of Electronics & Electrical Engineering, University of Wollongong Malaysia, Glenmarie Campus,40150, Shah Alam, Selangor, Malaysia.
[3]Department of Mechanical Engineering, University of Wollongong Malaysia, 40150, Shah Alam, Selangor, Malaysia.
[4]Department of Chemical & Petroleum Engineering, Faculty of Engineering, Technology and Built Environment, UCSI University, Malaysia.
[5]Department of Electrical and Electronics Engineering, School of Engineering, University of Wollongong Malaysia Penang, Jalan Anson, 10400, George Town, Pulau Pinang
*Corresponding author: Mohammed JK Bashir. E-mail: jkbashir@utar.edu.my

Graphical abstract:

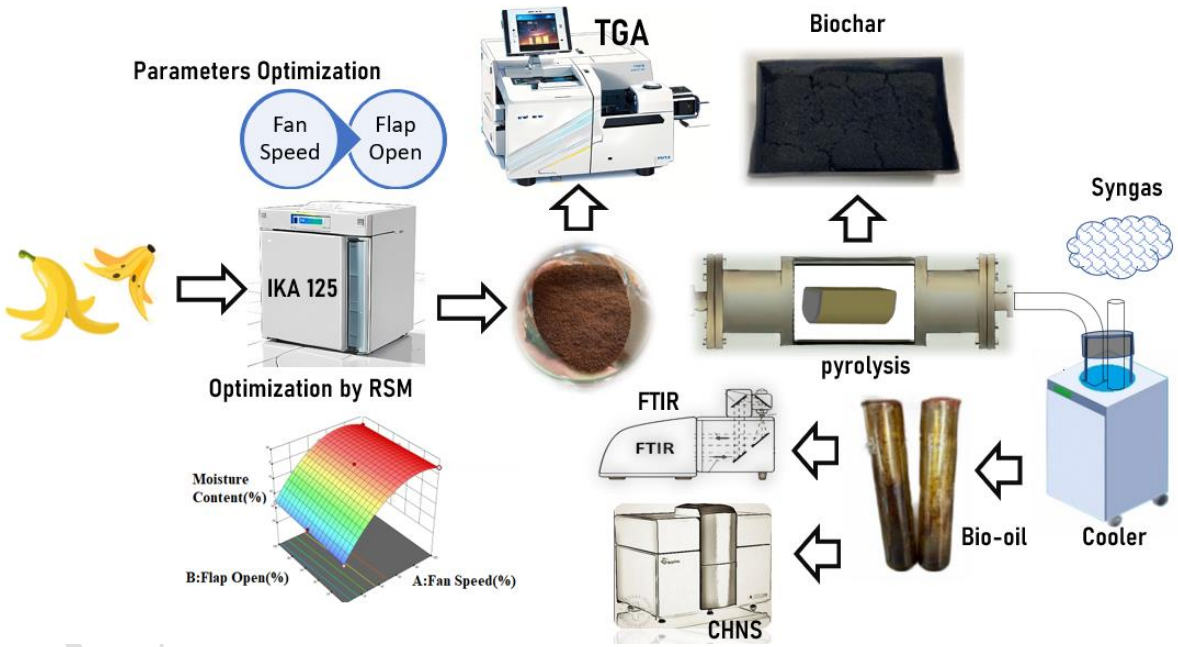

ABSTRACT

Banana waste has a high level of volatile matter, making it a promising feedstock for pyrolysis in bio-oil generation. Thus, an oven drying method optimization study was conducted to find the drying process of Saba banana peel on flap opening and fan speed. Based on the ANOVA results, it was found that the drying process using 60% fan speed and 40% flap opening for 6 hours of drying time could remove 84.07% of the moisture content

from the banana peel. Differential thermal analysis (DTA) was employed to characterize dried banana peels. The TGA study showed that the volatile matter concentration of the dried banana peels was 76.47% when using the ASTM drying method and 70.95% when using the improvement parameter optimization for the drying process. The bio-oil's high heating value (HHV) at 300 °C was 38.88 MJ/kg. The yields of bio-oil, biochar, and syngas obtained from the pyrolysis process were 16.6%, 36.45%, and 46.96%, respectively. The carbon hydrogen nitrogen sulfur (CHNS) ultimate analysis study showed a bio-oil elemental composition of 65.59% carbon, 8.27% hydrogen, 2.94% nitrogen, 0.93% sulfur, and 22.27% oxygen. Fourier transform infrared (FTIR) spectroscopy showed that functional groups including alcohol, alkane, phenol, and primary alcohol are present.

Keywords: Banana Peel; CCD Optimization; Pyrolysis; Proximate Analysis; Ultimate Analysis

1. Introduction

The country's urbanization and economic growth lead to more waste generation. By 2050, it is projected that there will be a substantial increase of 73% from the levels observed in 2020, reaching a staggering 3.88 billion tonnes. Mismanagement of municipal solid waste (MSW) can cause serious health, safety, and environmental problems. Thus, it is important to actively pursue alternative solutions that can transform MSW into valuable resources. To reduce environmental impact, Malaysia can reduce landfill reliance and harmful emissions (Shehzad et al., 2016) One potential solution is the utilization of MSW for energy generation, such as incineration. MSW incineration can be beneficial as it can significantly reduce the weight (up to 75%) and volume (up to 90%) of MSW (Chua et al., 2019). Pulau Langkawi, Pulau Tioman, Pulau Pangkor, Cameron Highlands, and Pulau Langkawi, are among the five tourism locations that have five small-scale rotary kiln-type incinerators constructed.

Unfortunately, it did not successfully implement a few plants due to various reasons, including non-compliance with environmental impact assessment standards by the incinerator operators, inadequate local expertise and operators, as well as higher costs for incinerator maintenance and parts (Yong et al., 2019). The excessive moisture content of the MSW is one of the reasons for the incineration operation's failure. As a result, prior to incineration, the moisture content of the MSW must be reduced. (Chua et al., 2019). The disposal of food waste in landfills is a common practice in Malaysia, which is not environmentally sustainable (Yong et al., 2020). The issue of food waste is thus a pressing concern in Malaysia, requiring sustainable solutions to mitigate its environmental and social impacts. In this research, it used banana peel as a feedstock. Banana cultivation areas in Malaysia increased from 28,036 to 30,455.45 hectares between 2016 and 2018 (Onsang et al., 2023). Banana inflorescence bract waste (Bharathi & Jacob, 2023) has significant cellulose and hemicellulose content for second-generation biofuel production. For every 100 kilograms of fruit harvested, four tonnes of waste were produced. Pyrolysis is a thermal cracking process that involves exposing a feedstock material to high temperatures in the absence of oxygen, yielding valuable products such as bio-oil, biochar, and syngas. The literature on pyrolysis of banana peel for energy generation has a gap in knowledge concerning the optimal parameters for the drying process, as most studies have used a drying time of 16 to 24 hours under the ASTM E1757-19 standard (López et al., 2021). Exploring other factors in addition to the ASTM standard pre-treatment can reduce the drying time for banana peels. There is a limitation of data on the improvement of feedstock used in the drying process prior to pyrolysis. Consequently, this study investigates the characteristics of banana peel bio-oil between the ASTM standard and the newly proposed method. The banana peels were pre-treated using a fixed-bed thermal drying oven, IKA 125, based on the ASTM standard, while improvement method by varying flag and fan settings. The central composite design (CCD) was used to find the optimal

drying moisture based on the results obtained from the experiments. After being treated, banana peels become a feedstock that may be used in the following process. Subsequently, it will be grounded, sieve and subjected to pyrolysis process. In order to observe any characteristic changes, TGA, DTA, CHNS, and FTIR analyses were used to study optimal methods implementation.

2. Materials and methods

Figure 1 shows a schematic illustration of the project flowchart. The main experimental study involves drying banana peels for 16 hours to 24 hours according to ASTM standards (Selvarajoo & Hanson, 2014)(Soetardji et al., 2014)(Omulo et al., 2019). Another experimental study involves using the design expert software to suggest a combination of two (2) parameters for achieving maximum moisture content removal. The dried feedstock was grounded into fine particles measuring 0.2 mm using an electric vibrator sieving machine from Xinxiang Chenwei Machinery Co. Ltd. in China. The particle was chosen for use in the subsequent pyrolysis process. Biochar was collected and characterized through Mettler Toledo TGA/DSC1 thermogravimetric analysis from Mettler-Toledo (M) Sdn. Bhd. in Malaysia. Bio-oil was collected and characterized through ultimate analysis (CHNS) TruSpec Machine from LECO Instrument (M) Sdn. Bhd., Malaysia and Perkin Elmer 2000 FTIR spectroscopy-UTAR-Fsc Kampar-Perak-Malaysia, respectively.

2.1. Preparation of banana peel waste biomass

Saba banana, also known as Abu Nipah which is a vigorous clone, particularly popular in Malaysia. The peel waste, was collected from Pisang Goreng Crispy, a food stall in Shah Alam, Malaysia, to be used as the feedstock in this project. The banana peels were collected from their original waste source and transported to the point of disposal. The collected

banana peels were stored at room temperature in the lab for 1-3 days to maintain their consistency. After being dried, the banana peel underwent sieving in accordance with ASTM C136 (C136/C136M-14:, 2019).

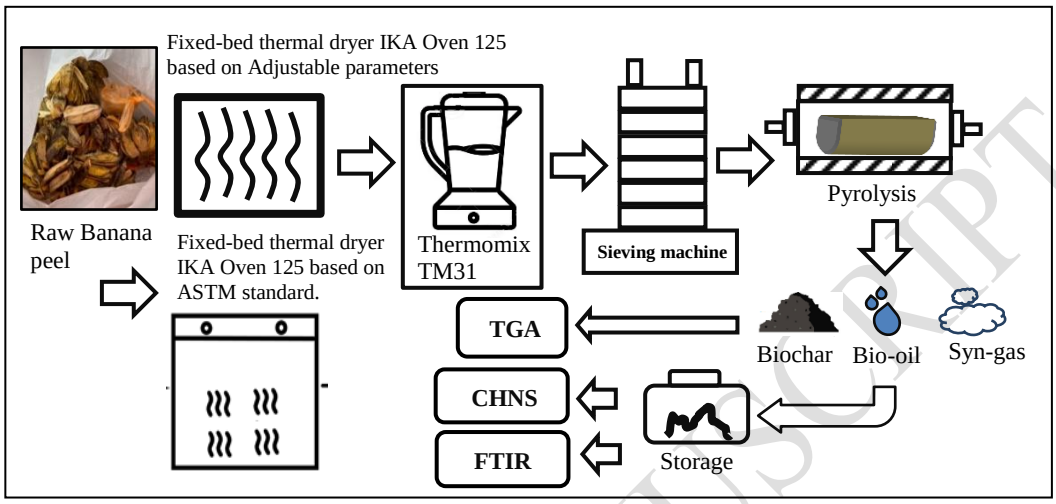

Figure 1: Schematic diagram of the project flowchart

2.2. Hardware set up description

The drying was done in an IKA Oven 125 Control-Dry, IKA Works Asia Sdn. Bhd., Malaysia, as shown in Figure 2, with different percentages of fan speed and flap opening. The grinding and sieving processes were performed using a Thermomix TM31, Thermomix Malaysia | True Mix Sdn. Bhd., Malaysia. The weight of banana peel was measured using a Mettler Toledo weighing scale from Mettler-Toledo (M) Sdn. Bhd. in Malaysia. For the pyrolysis process, a lab-sized fixed-bed thermal pyrolysis tube reactor was custom-built. Bomb calorimeter (IKA C200)-UTAR-Fsc-Kampar-Perak-Malaysia, is used to determine the value of Higher Heating Value (HHV).

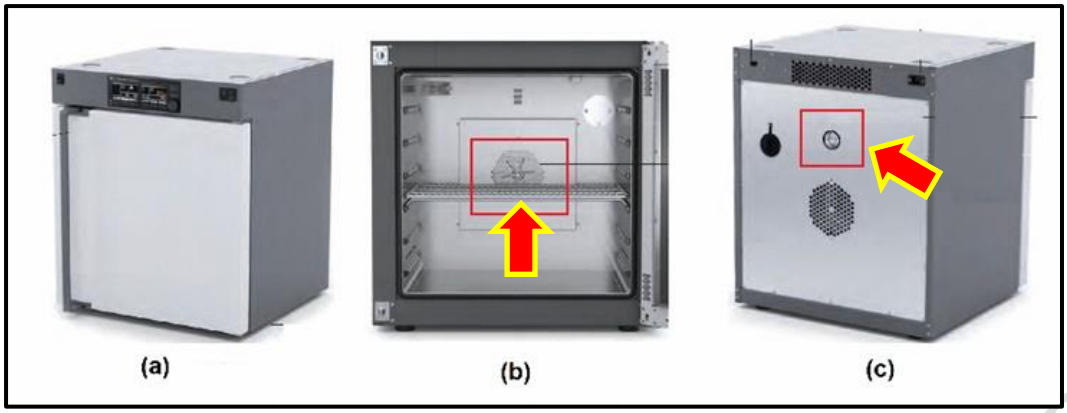

Figure 2: IKA Oven 125 (a) front view, (b) fan speed and (c) backside flap opening.

2.3. Initial moisture content analysis

The ASTM E-871 standard method (Kumar et al., 2020) was used to find the moisture content. The high moisture content affects the biochar (Taib, R. M. et al., 2021), and more thermal energy is necessary to vaporize the water present during the pyrolysis process. (Kabenge et al., 2018). The moisture content was calculated using Equation 1, and initial dry feedstock was calculated by deducting the initial dry weight of the feedstock from the initial wet weight of the feedstock

$$\textit{Initial Moisture content (MC\%)} = \frac{W1-W2}{W1} \times 100 \quad (1)$$

where, $W1$ is the wet weight of banana peel and $W2$ is the dry weight of banana peel after the heating pre-treatment.

2.4. ASTM standard moisture content analysis

The study followed the ASTM standard for drying one (1) Kg banana peel (BP) feedstock. The drying process was maintained at a constant temperature of 103 ºC ± 5 ºC, used a fan speed of 100%, and kept the flap open parameter at 0% for 16 hours. The mass of BP was measured at one-hour intervals. The drying process used different masses of banana peel, and

the mass of each feedstock was measured hourly to examine the trend in moisture content removal until a constant mass was achieved. The study used 300g, 750g, 1000g, and 2000g masses of banana peel, aiming to identify the optimal time required for each mass to reach a constant mass during the drying process. This drying process was carried out in order to prepare a dried banana peel (DBP) for the purpose of proximate analysis and pyrolysis.

2.5. Drying process experiment optimization

During the drying process of one (1) kilograms of banana peel at a constant temperature of 103ºC ± 5 ºC using different parameter settings for fan speed and flap opening, and the mass of BP was measured at one-hour intervals. The Response Surface Methodology (RSM)'s Central Composite Design (CCD) was carried out using the Design Expert. A total of 13 experiments were generated with a variation parameter of fan speed and flap open at constant temperature and drying time. This drying process was carried out in order to prepare a dried banana peel (DBP) for proximate analysis and pyrolysis process.

2.6. Proximate analysis through thermogravimetric analysis (TGA)

For centuries, according to Demirbas (2004), the ASTM standard methods E-872, D-1102, and E-871 were used to determine the contents of volatile matter, ash, moisture, and fixed carbon. In order to estimate the biomass's proximate analysis data with an average experimental error under 6%, the TGA approach (Garca et al. 2013) was recommended. The Mettler Toledo TGA/DSC1 was utilized to generate the TGA curve, which was then analyzed in the DBP to determine the moisture content, hemicellulose, cellulose, and lignin (volatile matter) composition, and the char formation. The ideal proportion of hemicellulose and cellulose in bio-oil for fuel application must be kept in mind. Because it has a larger energy content and can be transformed into liquid fuels more easily, cellulose-rich bio-oil is frequently chosen for fuel applications. Many researchers focused on the raw material of

banana peel for the TGA test. Two DBP samples of biochar were analyzed, one consisting of the DBP biochar using the ASTM standard, and the other consisting of the DBP biochar under the optimized drying parameter. According to Azariah (Pravin Kumar et al., 2022), the temperature rate of DBP is not much affected by the results of TGA. For the experiment, the DBP bio-oil was weighed at about $20\,mg \pm 1mg$ and placed into the auto-sampling machine holder. When increasing the temperature from ambient to 900 °C, a nitrogen gas flow of 50 ml per minute and a heating rate of 10 K per minute (1 °C per minute) were used. Thermal decomposition curves and differential thermogravimetric curves (DTA) (in the presence of N_2 gas flow) were used to characterize the DBP biochar. The following equations (Ali et al., 2020) were used to calculate the results of moisture, volatile matter, ash, and fixed carbon.

$$\text{Moisture content } (W_{m)}\ (\text{mg}) = \text{taken from the TGA graph at } 139°\text{C}\,.$$

$$\text{Volatiles } (W_{m)}\ (\text{mg}) = \text{taken from the TGA graph at } 900°\text{C}.$$

$$\text{Fixed carbon } (F_c) + \text{Ash } (W_{Ash})(\text{mg}) = \text{taken from the TGA graph at Residue.}$$

$$W_{Ash}(\text{mg}) = W_{org} - (W_m + W_v + F_c) \quad (2)$$

Where, mg is milligram, W_{org} is a original weight after the initial drying process, W_m is moisture content from the TGA graph below 139.45 °C (stage 1), W_v is volatile matter from the TGA graph from 139°C to 900°C, and F_c is fixed carbon. All the units in mg. To find the ash, the temperature is held at 900°C for 300 seconds (5 minutes) in the presence of N^2. The atmosphere will then change from N^2 to O^2, starting the combustion process until 950°C. Depletion of fixed carbon has been detected by this stage. Additionally, the total amounts of moisture, fixed carbon, and volatile matter are deducted from 100 in order to calculate the DBP's ash content. The fixed carbon was calculated by subtracting the sum of the others from the entire sample. The wt% denotes weight measurement as a percentage. The sum of Fixed

Carbon and Ash Content is equal to the difference between 100 and the sum of Moisture Content and Volatile Matter Content.

2.8. Ultimate analysis (CHNS)

The DBP bio-oil was performed CHNS elemental analysis. The compound results of the bio-oil, namely carbon (C), hydrogen (H), nitrogen (N), oxygen (O), and sulfur (S), were characterized in accordance with ASTM D3178. The higher heating values (HHV) values that were determined were validated through the application of the Luo and Resende (2014) principle, which involves utilizing the elemental percentages derived from ultimate analysis data (as shown in Equation 3). The estimation method and bomb calorimeter (IKA C200) were used to determine the value of Higher Heating Value (HHV). To get the percentage of oxygen, remove the total of the percentages of carbon, hydrogen, nitrogen, and sulfur from 100%. To calculate the Low Heating Value, subtract the product of the Higher Heating Value (HHV) and the higher heating value of water vapor (Hv) from the product of the molar weight (Mw) of water vapor. Hv is the heat of vaporization of water (usually taken as 44,000 kJ/kg), Mw is the moisture content of the fuel between 10% to 30% (expressed as a decimal fraction, 0.15). The determination of lower heating values (LHV) of the samples was carried out by applying equation 4. This equation used the higher heating values (HHV) and hydrogen contents of the samples, following the method outlined by Kabenge, Isa, et al., 2018. The computation of oxygen percentage (O%) was calculated through the deduction of the combined percentages of carbon, hydrogen, nitrogen, and sulfur from 100%, as shown in the following equation 5:

$$HHV\left(\frac{MJ}{kg}\right) = \%C \times 0.3578 + \%H \times 1.1356 + \%N \times 0.0594 - \%O \times 0.0854 - 0.974 \quad (3)$$

$$LHV_{dry} = HHV_{dry} - 2.442\left(\frac{8.936\mathrm{H}}{100}\right)\mathrm{MJ/kg} \quad (4)$$

$$\%O = 100\ \% - (\%C + \%H + \&N + \%S) \quad (5)$$

2.9. Fourier-transform infrared (FTIR) spectrometer analysis

The Fourier-Transform Infrared (FTIR) spectrometer was used for the analysis the chemical compound of extracted bio-oil is the Perkin Elemer 2000-Fourier Transform Infrared spectrometer, which is able obtaining the wavelength range of 4000 cm^{-1} to 400 cm^{-1}. It's important to note that the FTIR spectrum of a given molecule will be more complex than just these functional group absorptions, and additional peaks and features may be present depending on the specific molecular structure and environment.

2.10. Pyrolysis process

Figure 3 shows the schematic of the fixed bed thermal drying reactor and was utilized to carry out the slow pyrolysis process for extracting bio-oil from the feedstock. A mass of 80g of feedstock was placed on a metal basket and inserted into the reactor, followed by securely closing the front and back of the reactor to prevent any air from entering the system. The DBP that had been dried had a moisture content between 6.7 and 11.6% (Kabenge et al., 2018), which is suitable for biomass slow pyrolysis requirements. Prior to initiating the slow pyrolysis process, the reactor was filled with nitrogen gas at a constant flowrate of 0.5 l/min. Subsequently, the parameters of the pyrolysis process, such as the temperature, heating rate, and residence time were set through software at 300 ºC, 10 ºC/min, and 90 minutes, respectively. The resulting hot gas from the reactor was directed into a test tube placed in the condenser to collect and condense the gas into bio-oil. After the completion of the pyrolysis process, the mass of the bio-char and bio-oil mass were measured, and the percentage of pyrolysis product yield was calculated using formula below:

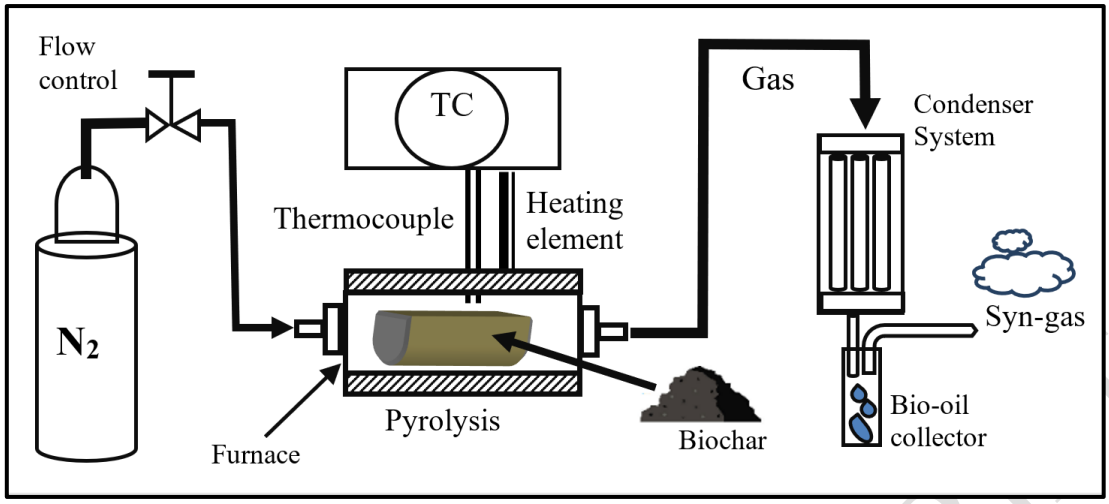

Figure 3: Schematic diagram of fixed-bed thermal drying reactor.

$$\text{Biochar yield, wt\%} = \frac{\text{Mass of Bio-Char (g)}}{\text{Mass of Dry feedstock}} \times 100\% \quad (6)$$

$$\text{bio} - \text{oil yield, wt\%} = \frac{\text{Mass of Bio-Oil (g)}}{\text{Mass of Dry feedstock}} \times 100\% \quad (7)$$

$$\text{Percentage of syngas yield, wt\%} = 100\% - \%\text{biochar} - \%\text{bio} - \text{oil} \quad (8)$$

2.11. Pyrolysis process

The central composite design (CCD) of design expert approach (Ivanova et al., 2016), an experimental design technique, has become increasingly popular for optimizing processes due to its convenience and effectiveness (Bashir et al., 2011). It is possible to generate a quadratic model for response variables without conducting a minimum of two-level factorial experiment, using a technique known as second-order modeling. A CCD experiment can be created using two levels (+1 and -1) for factors, which is equivalent to a full factorial design represented by 2n. The experiment can be repeated n_c times to minimize errors. The total of the experiment runs is calculated by:

$$N = 2^n + 2n + n_c \quad (9)$$

Where n denotes the number of factors, while n_c denotes the number of tests that must be carried out repeatedly. There were three levels for each variable that were looked at +α, 0 and –α. The α value can be determined using the following equation 10:

$$\alpha = (2^n)^{\frac{1}{4}} \quad (10$$

There are five (5) replications that must be carried out repeatedly based on the equation 9 and a total of 13 runs were carried out.

3. Results and Discussion

3.1. ASTM standard of pre-treatment of drying process

The result of the moisture content of the feedstocks were measured using the following formula one (1). Figure 4 shows that the trend in moisture content for different masses of banana peel feedstock during the 16-hour drying process according to the ASTM standard. The results indicate that the optimal 16 hours duration for achieving constant mass of banana peel feedstock in 300g, 750g, 1000g, and 2000g of drying process with 80.57%, 83.35%, 84.03%, and 80.79% respectively. The experiment demonstrated that a length of 16 hours was ideal for keeping a constant mass during the drying phase of banana peel feedstock. The results were consistent across different quantities of 300g, 750g, 1000g, and 2000g. These findings give useful insights into the 16-hour pre-drying process of banana peels weighing 300g to 2000g.

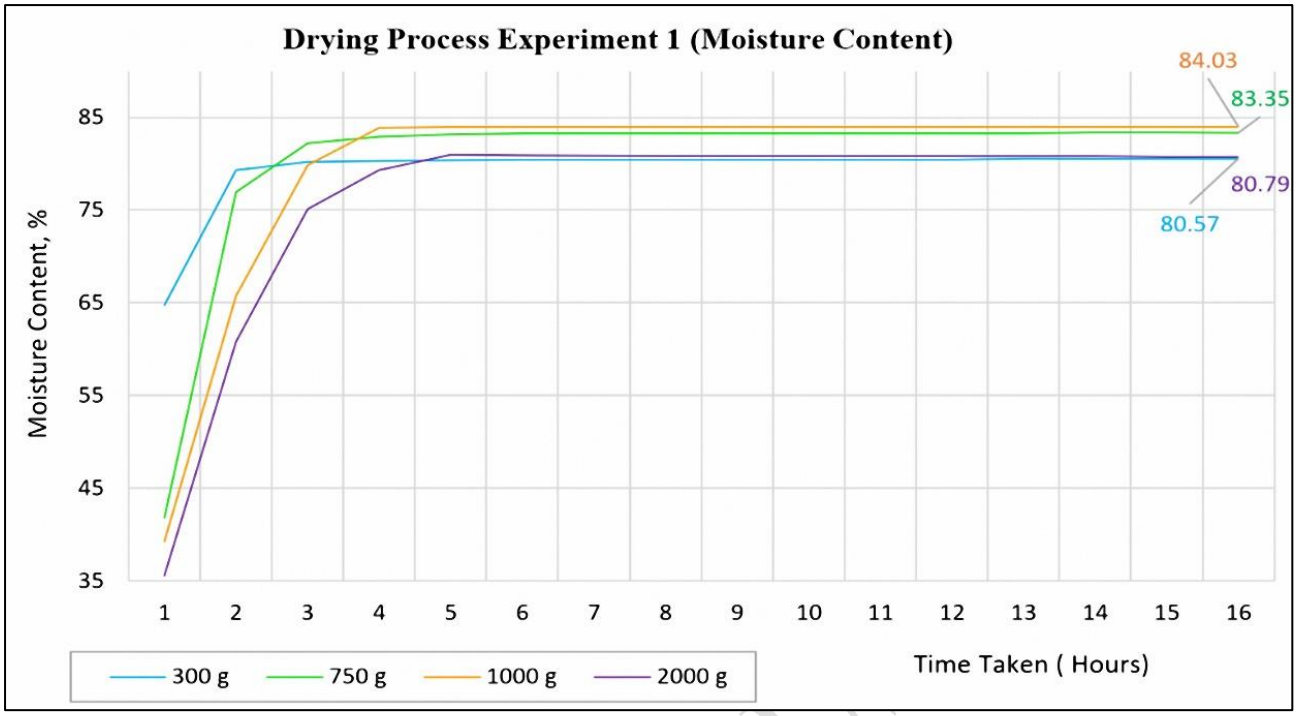

Figure 4: Moisture content of drying process based on ASTM standard.

3.2. Optimization method of pre-treatment of Drying Process Experiment

Table 1 shows two (2) independent variables that were manipulated in this study to investigate their impact on the response variable of moisture content removal (Y) were the oven fan speed (A) and flap open (B). Thus, the α (Eq.10) is equal to 1.4142. Due to limitation of fan speed and flap open, α value was set to 1.

Table 2 shows the resulting data from the 13 experiments were entered into the RSM for optimization and presents the design matrix generated by the software, which includes the fan speed and flap open values, as well as the predicted and actual moisture content values. Based on the optimal parameters for the drying process were determined to be 60% fan speed and 40% flap open.

Table 1: Selection of independent variables for optimization of moisture removal

`	Coding	Unit	Level			
			Low	***High***	$+\alpha$	$-\alpha$
Fan speed	A	%	0	100	0	100
Flap open	B	%	0	100	0	100

Note: α, the distance from the centre point was set at 1

Parameter: Temperature (105°C ± 5°C), Drying time: 6 hours					
Run	(A) Fan Speed (%))	(B) Flap Open	Final Mass(gram)	(Y) Moisture content (%)	
				Actual	Predicted
1	0	0	497.0	50.30	50.33
2	0	50	470.9	52.12	52.77
3	0	100	455.7	82.06	54.54
4	50	0	179.4	82.06	82.19
5	50	50	165.3	83.47	83.47
6	50	50	163.2	83.68	83.68
7	50	50	167.1	83.29	83.29
8	50	50	165.1	83.49	83.49
9	50	50	169.1	83.09	83.09
10	50	100	169.1	83.91	83.91
11	100	0	152.8	84.72	84.55
12	100	50	157.8	84.22	84.49
13	100	100	161.2	83.88	83.78

Table 2: Moisture Content responses from CCD experiment parameters

3.3.RSM optimization study of moisture content reduction yield

Table 3 shows the results of the analysis conducted on the fit summary generated by the Design Expert software. According to the guidelines, a sequential p-value that is lower than 0.05 is considered significant. Comparing the sequential p-values of each source model, only the quadratic model has a significant value with a sequential p-value lower than 0.0001. Additionally, a lack of fit p-value higher than 0.1 is preferred, as a higher p-value indicates weaker lack of fit (Bashir et al., 2011). The quadratic and cubic models both have lack of fit p-values above 0.1, with values of 0.9997 and 0.9540, respectively. A high R^2 value is also desirable, with the difference between the adjusted and predicted R^2 values being lower than 0.2. The quadratic model has a high R^2 value, and the difference between the adjusted and predicted R^2 values is 0.0006, which is lower than 0.2. Therefore, the software recommends the quadratic model as the suggested model. However, the cubic model is considered aliased and not recommended due to insufficient runs to estimate all the coefficients of the model. The standard deviation for the model shows that the amount of the random variation left in

the process is 0.1690. Therefore, the value of the predicted R^2 of this model is 0.9999 which is in significant value with the adjusted R^2 of 0.9998. The difference between predicted adjusted R^2 is lower than 0.2. An acceptable value for the signal-to-noise ratio is one that is larger than 4, which may be measured with sufficient accuracy. Table 4 shows the results of the coefficient analysis of variance (ANOVA) for the quadratic model generates by Design Expert software. The overall quadratic model consists of 5 degrees of freedom model which are the fan speed (A) and flap open (B). The condition of the module is in significant state as the p-value of the model is 0.0001 and the F-value is 15673.53. Therefore, the lack of fit p-value is not significant which is showing a good value for it and the value of the lack of fit p-value is 0.9997, larger than 0.1. The lack of fit F-value was 0.003, which shows the lack of fit is not significant relative to the pure error. A non-significant lack of fit is indicative of a good fit in the model, given the probability of the occurrence of such a large Lack of Fit F-value due to noise is 99.97%. All the individual term of the model includes of A, B, AB, and A^2 are in a significant p-value

Table 3: Fit summary of moisture content

Source	Linear	2FI	Quadratic	Cubic
Sequential *p*-value	0.0035	0.7854	**<0.0001**	0.9965
Lack of fit *p*-value	<0.0001	<0.0001	**0.9997**	0.9540
Adjusted R^2	0.6121	0.5727	**0.9998**	0.9998
Predicted R^2	0.3610	-0.3151	**0.9999**	0.9999
			Suggested	Aliased

Table 4: Coefficient analysis of variance (ANOVA) for quadratic model.

Sources	Sum of squares	Degree of freedom (df)	Mean square	*F*-value	*P*-value	
Model	2238.98	5	447.80	15673.53	<0.0001	significant
A-Fan Speed	1510.82	1	1510.82	52881.20	<0.0001	
B-Flap Open	4.49	1	4.49	157.13	<0.0001	
AB	6.28	1	6.28	219.64	<0.0001	
A^2	602.19	1	602.19	21077.73	<0.0001	
B^2	0.3307	1	0.3307	11.58	0.0114	
Residual	0.2000	7	0.0286			
Lack of Fit	0.0005	3	0.0002	0.0031	0.9997	not significant
Pure Error	0.1995	4	0.0499			
Corelation Total	2239.18	12				

which the p-value is lower than 0.1 and there is no need to conduct the model reduction for the model. The results did not utilize model reduction to remove the B^2. The p-value that is higher than 0.1 indicate the model term is not significant (Bashir et al., 2011). Besides, the quadratic model shows that A and A^2 terms which are the fan speed factor and the fan speed quadratic model have significant and higher F-value of 52881.20 and 21077.73. The coded equation for moisture content of DBP is shown in equation 11, while the actual equation for moisture content DBP is shown in equation 12 where A and B are representing fan speed and flap open.

$$\boldsymbol{Predicted\ Moisture\ Content}\ (\%) = 83.40 + 15.85(A) + 0.8650(\mathrm{B}) - 1.25(\mathrm{A})(\mathrm{B}) - 14.77(A^2) - 0.3460(B^2) \quad (11)$$

$$\boldsymbol{Actual\ Moisture\ Content}\ (\%) = 50.30382 + 0.933058(A) + 0.056191(B) - 0.000501(A)(B) + 0.005906(A^2) - 0.000138(B^2) \quad (12)$$

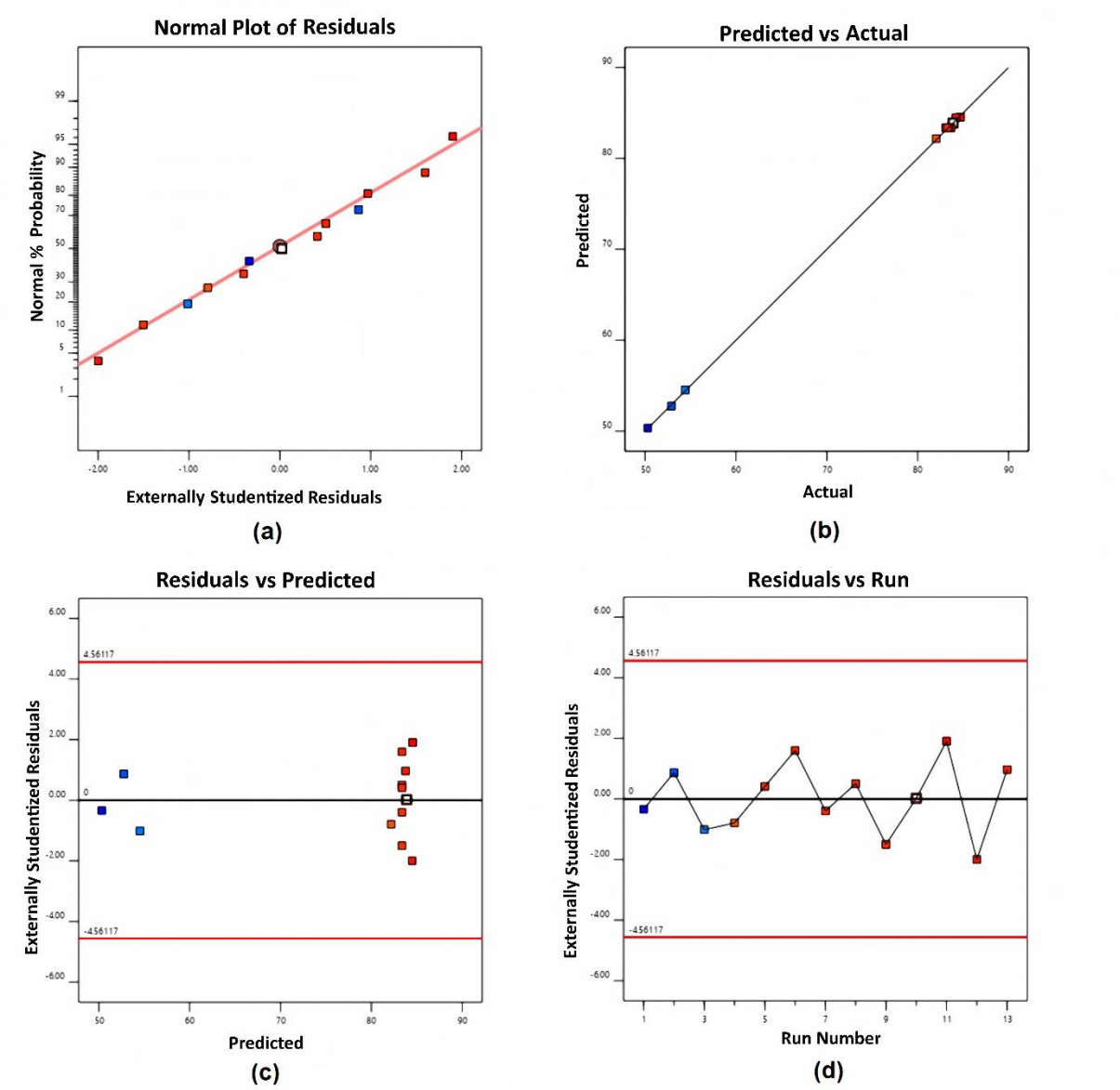

Figure 5: Diagnostics data for (a) Normal Plot of Residuals, (b) Predicted vs Actual, (c) Residual vs Predicted and (d) Residual vs Run plots.

The results of the normal plot of residuals, predicted vs actual, residual vs prediction graph, and residual vs run graph are shown in Figure 5(a)-(d). These graphs demonstrate that the performance of each diagnostic meets the requirements of ANOVA, indicating the validity of the ANOVA model. Figure 5(a) presents the normal plot of residuals for the model. The plotted points of the residuals are roughly distributed along the red straight line, indicating a good fit of the model to the normal distribution. Figure 5(b) presents the diagnostic plot for predicted versus actual values. The plot indicates a strong agreement between the predicted

and actual values, as the points are closely distributed near the straight line with a slope of 1. This suggests that the model has a good level of accuracy and consistency in its predictions. Figure 5(c) displays the residual vs predicted graph, where all the data points fall within the threshold range of ± 4.56117 (red line) and are distributed closely around the zero line. There is not any pattern in the plot indicates that the model fit is valid. The graph in Figure 5(d) displays the residual plotted against the run. All the points fall within the threshold range of ± 4.56117 (red line) and are scattered around the zero line with no discernible pattern. These observations suggest that the model fit is valid. Figure 6 illustrates the optimization process to determine whether A or B can produce optimal results. Design Expert numerical optimization offers the flexibility to select maximum, minimum, or target values from a single response or combination of responses as optional choices. The moisture content was selected to achieve the maximum weight loss, while ensuring that A and B remained within the specified range (The column was chosen in range). According to the suggestions from Design Expert software, the parameters identified for achieving the maximum moisture content in the model were a fan speed of 85.639% and a flap opening of 38.960%. The model for fan speed was rounded up to 86%, while the flap opening model was rounded up to 39%. The response of moisture content recalculated and it was produced the 84.55%. Figure 7 shows the effect percentage of the flap opening and fan speed. The impact of flap opening parameter on moisture content removal from feedstock was studied, and the findings indicated that there was a low significant effect. The data did not support a lot on the hypothesis for the moisture content removal. The lowest percentage range of moisture content removal was observed at 0% flap open, whereas the highest percentage range was observed at 50% and 100% flap opening, suggesting that lower flap opening percentages are less effective at removing moisture. The fan speed had a significant impact on moisture content removal, with increasing fan speed leading to higher moisture removal. The

experiment found that there was a substantial improvement in moisture removal as fan speed was increased up to a certain point at 80%, but beyond that point, the percentage increment in moisture removal decreased.

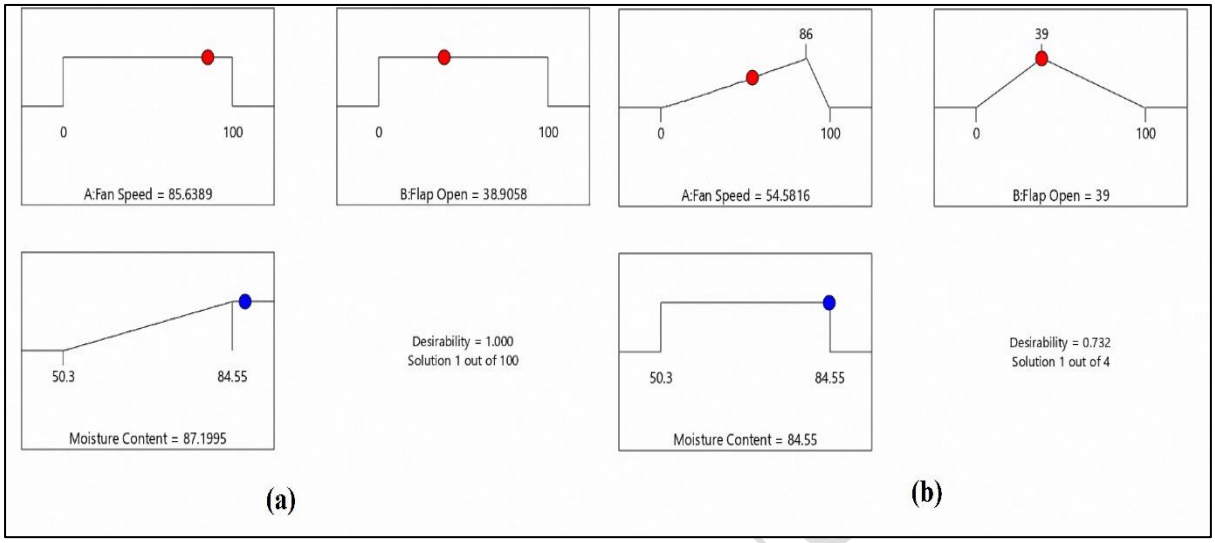

Figure 6: Suggested parameter of the model (a) initial proposed by Design Expert and (b) rounded up A and B.

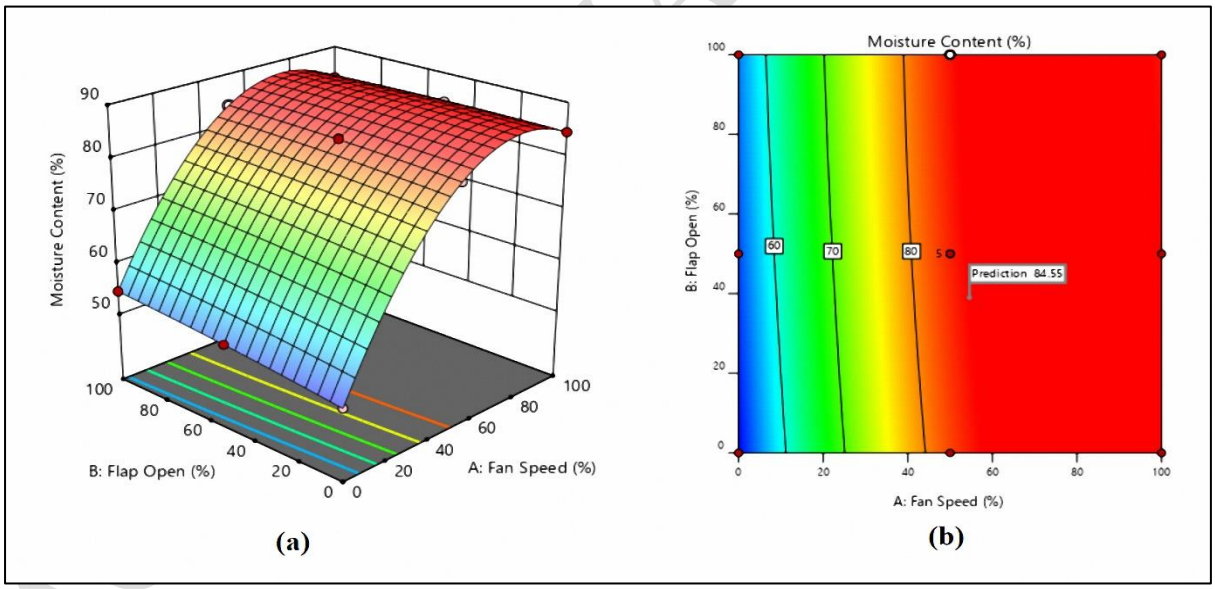

Figure 7: Model graph (a) Effect of 3D Model of fan speed and flap open on the moisture content and (b) its contour plot

3.4. Biochar proximate analysis using thermogravimetric analysis (TGA)

Figure 8 shows how the weight percentage of DBP feedstock changed as temperature increased from room temperature to 900°C in the presence of nitrogen. The DBP feedstock being dried for 16 hours according to ASTM standard. The curve exhibits three significant weight losses. The first weight loss of -3.44% (20.3458 mg) occurred between 50°C to 139.45°C, indicating the evaporation of moisture content. The volatile matter content of biomass decreased during thermal degradation in second stage. This process involved the degradation of cellulose, hemicellulose, and lignin fractions. The graph shows a weight decrease that caused the differential thermogravimetric curve (DTA) curve to reach its lowest point. The second weight loss occurred between 139.45°C to 565.64°C, with approximately -64.65% (6.7258 mg) of the sample's contents being evaporated. This occurred because it released the volatile matter contents. While the third weight loss took place at a temperature above 565.74°C, causing the evaporation of -15.33% (3.4958 mg) of the sample contents. The residual material left after all contents had fully evaporated weighed +16.38% (3.45mg) and remained as solid char. Referring to the DTG curve, hemicellulose and cellulose initiated thermal decomposition around 299.55°C, with a devolatilization rate of 11.30 mg weight loss per minute. Tables 5 shows the results of proximate analysis using ASTM standard method. DBP has a volatile matter content of approximately 80%, consisting of high hemicellulose, cellulose decomposition, and lignin decomposition. Figure 9 shows how the weight percentage of DBP feedstock changed as temperature increased from room temperature to 900°C in the presence of nitrogen. The DBP feedstock being dried according to the CCD model are 60% fan speed and 37 % flap open for 6 hours. The curve exhibits three significant weight losses. The first weight loss of -2.83% (20.3102 mg) occurred between 50°C to 134.90°C, indicating the evaporation of moisture content. The volatile matter content of biomass also decreased during thermal degradation in second stage. This process involved the degradation of cellulose, hemicellulose, and lignin fractions. The second weight loss occurred between 136.75°C to 563.66°C, with approximately -61.93% (7.3702

mg) of the sample's contents being evaporated. This occurred because the volatile matter contents were released.

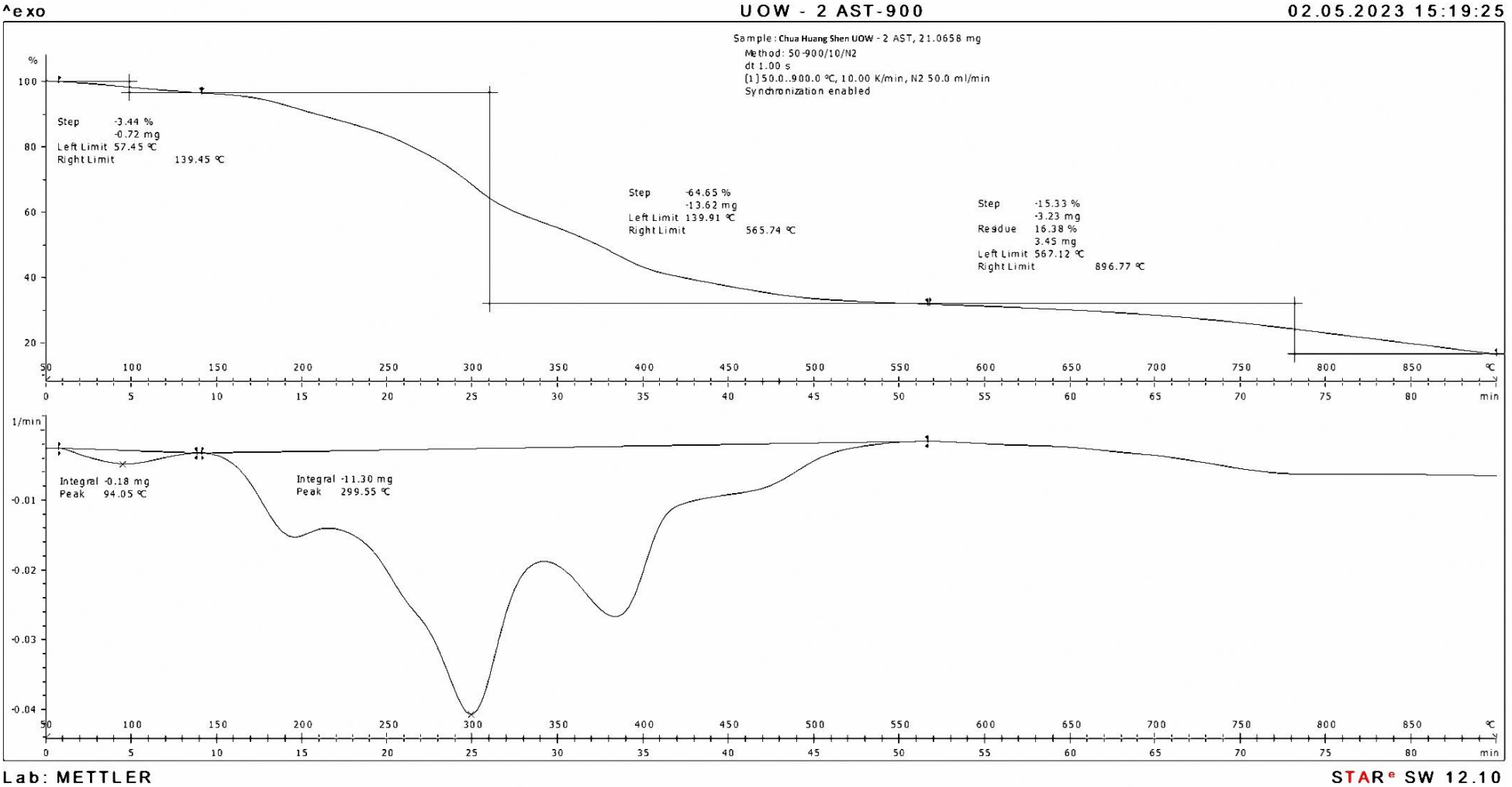

Figure 8: Thermogravimetric (TG) and derivative thermogravimetric (DTG) plots from ASTM standard.

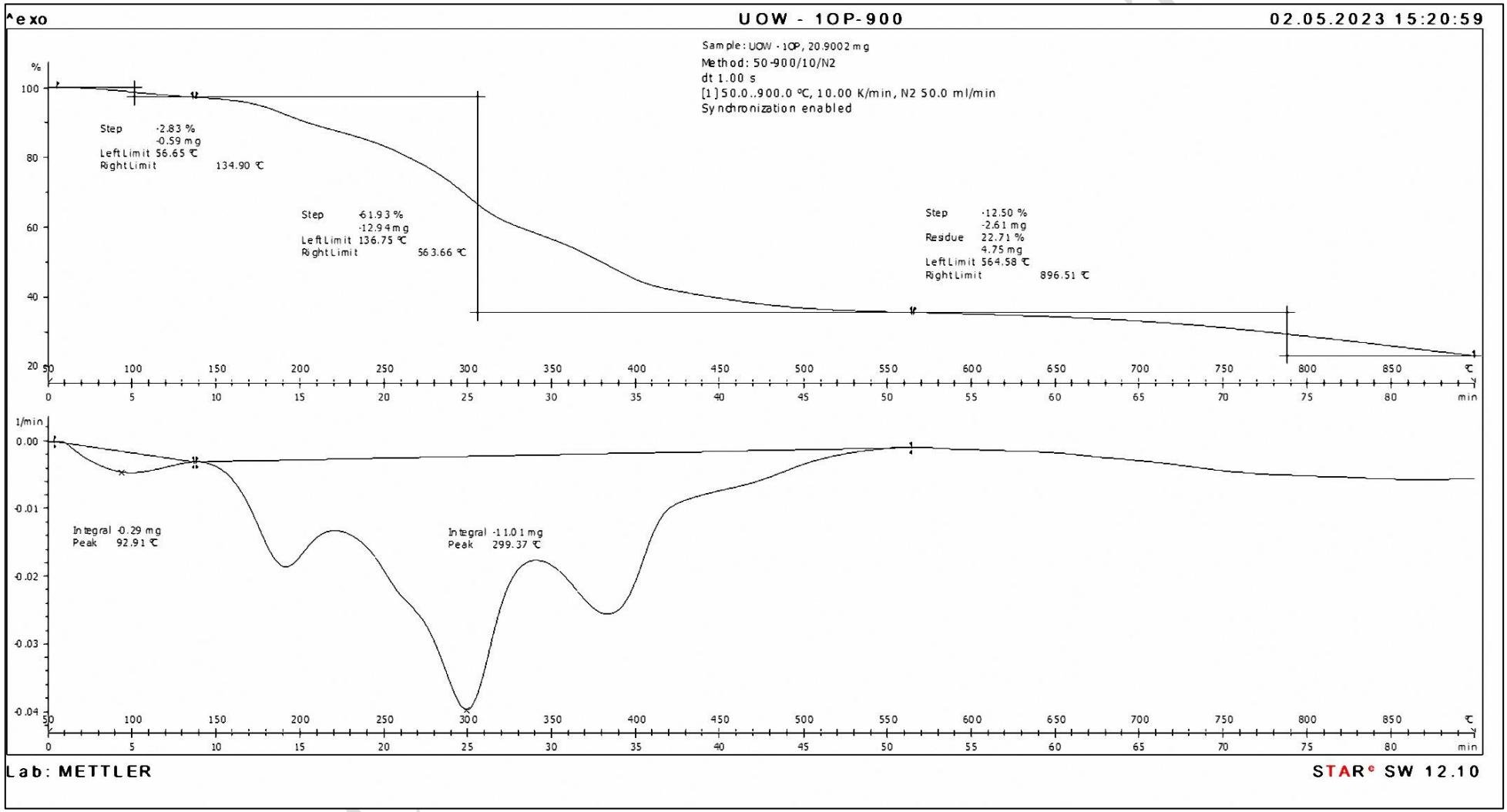

Figure 9: Thermogravimetric (TG) and derivative thermogravimetric (DTG) plots from optimization method.

While the third weight loss took place at a temperature above 565.74°C, causing the evaporation of -12.50% (4.7602 mg) of the sample contents. The residual material left after all contents had fully evaporated weighed +22.71% (4.75mg) and remained as solid char. According to the DTG curve, hemicellulose and cellulose began thermal decomposition at a temperature of about 299.37°C and a devolatilization rate of 11.01 mg of weight loss per minute. Tables 5 shows the results of proximate analysis using optimization method. DBP has a volatile matter content of approximately 80%, consisting of high hemicellulose, cellulose decomposition, and lignin decomposition. Nurhayati Abdullah, Isa, et al. (2018) used ASTM E872, ASTM E871-82, and ASTM D1102-84 standards to assess moisture content, volatile matter, and ash (entire sample), respectively. Omulo, Godfrey (Omulo et al., 2019) used the ASTM D5142 approach for proximate analysis in their investigation. Table 6 compares the proximal analysis of the different researchers. The proximate analysis findings from the ASTM technique and the optimization approach were compared, and the raw feedstock of DBP analysis indicated changes in volatile matter content, moisture content, ash content and fixed carbon. Differences in temperature ramps and weight loss against temperature are also reported.

3.5. Bio-oil Ultimate Analysis using CHNS Analysis

Table 7 shows the results of the CHNS analysis that was done to find out what kinds of elements were in the bio-oil pyrolyzed from dried banana peels using the optimization method and the ASTM standard method. The ultimate analysis showed that the bio-oil of DBP consisted very similar properties between the optimization method and ASTM standard method. The higher heating value (HHV) of the bio-oil was calculated to be 25.43 MJ/kg using a formula from a previous study (Kabenge et al., 2018). The analyzed high heating values (HHV) and low heating values (LHV) of BDP bio-oil are presented in table 5. The analyzed high heating values (HHV) and low heating values (LHV) of BDP bio-oil are presented in table 5. Generally, a higher HHV is desirable as it indicates a greater energy content in the bio-oil. Typical HHV values for bio-oil can

range from 18 to 24 MJ/kg. Table 7 compares the final analysis for bio-oil derived from various sections of the banana plant, specifically the banana peels, banana leaves, and banana peduncle.

Table 5: Moisture Content from ASTM and Optimization method Drying Process

	DBP feedstock (21.0658mg)		
	Proximate Analysis	**mg**	***wt.100%**
ASTM method	Moisture Content	0.72	3.42%
	Volatile Matter Content	16.85	79.99%
	Fixed Carbon + Ash Content	3.4958	16.59%
Optimization method	Moisture Content	0.59	2.83%
	Volatile Matter Content	15.55	74.40%
	Fixed Carbon + Ash Content	4.925	16.59%

Table 6: Comparison of Proximate Analysis

Type of Banana peel	**DBP Bio-oil**		**Banana peel raw feedstock**		
Proximate Analysis	**ASTM methos**	**Optimization method**	**Nurhayati Abdullah et. Al. 2015**	**Kabenge, Isa, et al 2017**	**Omulo, Godfrey, et al 2019**
Moisture Content	3.42%	2.83%	10.2%	11.56%	11.56%
Volatile Matter Content	79.99%	74.40%	80.6%	88.02%	88.02%
*Fixed Carbon + Ash Content	16.59%	22.73%	19.4%	11.98%	11.98%
Temperature ramps	1°C/min	1°C/min	10°C/min	15°C/min	None
First weight loss temperature	50°C to 139.45°C	50°C to 134.90°C	30°C to 122.50°C	50°C to 200°C	None
Second weight loss temperature	139.45°C to 565.64°C	136.75°C to 563.66°C	122°C to 619.96°C	200°C to 550°C	None
Third weight loss temperature	565.74°C to 900°C	565.74°C to 900°C	620.84°C to 907.74°C	600°C to 900°C	None

The information of Table 7 was gathered from a variety of sources, including the CCD optimization technique (DBP bio-oil), Isa Kabenge, Rahmad Mohd Taib and Aziz, and Arun, A. et al. The investigation focuses largely on the percentage composition of hydrogen (H), carbon (C), sulphur

(S), nitrogen (N), and oxygen (O) in the bio-oil samples, as well as the high and low heating values. The bio-oil from banana leaves has the maximum oxygen content, while the CCD optimised bio-oil has the highest levels of carbon, hydrogen, nitrogen, and sulphur. Furthermore, compared to bio-oil from

Table 7: Ultimate Analysis of bio-oil DBP CCD optimization method, ASTM standard and researchers

		CCD optimization method	**ASTM standard**	**B. Peels Isa Kabenge et al. (Kabenge et al. 2018)**	**B. leaves Rahmad Mohd Taib(Taib, Abdullah, and Aziz 2021)**	**B. Peduncle Arun, A. et al. (Arun, Velmuruga n, and Kumar 2018)**
Composition	**Symbol**	**Percentage**	**Percentage**	**Percentage**	**Percentage**	**Percentage**
Carbon	C	65.59%	69.12%	36.65%	55.9%	48.37%
Hydrogen	H	8.27%	7.83%	6.19%	7.8%	5.90
Nitrogen	N	2.94%	2.43%	1.94%	0.87%	0.76
Sulphur	S	0.93	0.82%	20.75%	0.08%	0.03%
*Oxygen	O	22.27%	19.80%	45.94%	35.3%	44.94%
High Heating Value (bomb calorimeter)	Calorific Value (MJ/kg)	38.88	36.42	16.15%	25%	N/A
High Heating Value (Estimation method)	Calorific Value (MJ/kg)	30.32	31.10	N/A	N/A	N/A
*Low Heating Value (bomb calorimeter)	Calorific Value (MJ/kg)	32.38	28.82	N/A	N/A	N/A
Low Heating Value (Estimation method)	Calorific Value (MJ/kg)	28.59	29.40	14.80%	N/A	N/A

other sources, the CCD optimised bio-oil has a much higher high heating value. The analysis of bio-oil samples from several sources, including the present banana peel (BDP), the banana peduncle (BP) (Arun, Velmurugan, and Kumar, 2018), and the banana pseudo-stem (BPS) (Taib, Abdullah,

and Aziz, 2021), reveals that each sample has unique chemical characteristics and functional groups.

3.6. Pyrolysis process.

Table 8 shows the results of the pyrolysis process, which generated biochar, bio-oil, and syngas. Hernan D. Lopez et al. conducted the optimization of bio-oil parameters for banana peel at 300 °C and a heating rate of 10 °C per minute. The temperature for both runs (ASTM method and optimization method) was 300°C, with a heating rate of 10°C per minute, a nitrogen (N^2) gas flow rate of 0.5 liters per minute, and a residence time of 90 minutes. The pyrolysis process produced an average total percentage composition of bio-oil, biochar, and syngas of 36.45%, 16.6%, and 46.96%, respectively. The optimization method produced a higher percentage of biochar and bio-oil than Hernan D. Lopez et al. The comparison of current data and published results for biochar, bio-oil, and syngas indicates significant composition changes. Table 8 compares current data on the composition of biochar, bio-oil, and syngas at various temperatures and heating rates to those published in 2021 by Hernan D. Lopez et al. and Rahmad Mohd Taib et al. The study is based on all products being tested at 300°C with a heating rate of 10°C per minute, with the exception of Syngas, which was measured at 500°C with the same heating rate. These variances might be ascribed to variations in experimental settings, feedstock properties, and the researchers' analytical procedures. It is recommended that the condensing system and procedure be improved to enhance the collection of bio-oil during the pyrolysis process. Currently, bio-oil is collected in a test tube, which is surrounded by water at 5°C to condense the gas into a liquid. However, this method is not as efficient as a multi-stage condensing system used in a research done by Sadegh Papari and Kelly Hawboldt (Papari and Hawboldt, 2018), which was shown to produce higher yields in collecting bio-oil. Table 8 shows that most reported results have high yields of bio-oil and biochar. It is recommended that the condensing system and procedure be improved to enhance the collection of bio-oil during the pyrolysis process.

3.7. FTIR Analysis.

Table 9 displays the FTIR data for slow pyrolysis-produced DBP bio-oil. The FTIR analysis result in Figure 10 demonstrates the presence of common functional groups in the DBP bio-oil. In region A, a broad peak was detected at 3414 cm^{-1} between 3600 cm^{-1} and 3200 cm^{-1} indicate the present of

Table 8: Output Product Composition from Pyrolysis Process and comparison

Pyrolysis Products	Percentage (%)		
	Current DBP	Hernan D. Lopez et. Al. 2021 (López, Ayala, and Malagón-Romero 2021)	Rahmad Mohd Taib et. Al. 2021(Taib, Abdullah, and Aziz 2021)
	(300°C, 10 °C/min)	(300°C, 10 °C/min)	(500°C, 10 °C/min)
Biochar	35.59	31.48	40.3
Bio-oil	15.08	6.43	39.4
Syngas	49.33	60.07	20.3

Table 9: FTIR functional group compositions of DBP.

Wave number range (cm^{-1})	Wave number (cm^{-1})	Group	Class of compound
3200-3600	3414	O-H bonded	alcohol and phenols
2850-300	2854, 2925	C-H stretching	alkane
1850-1650	1710, 1639	C=0 stretching	ketones, aldehyde, carboxylic acids
1600-1400	1455	C=C stretching	aromatic
1400-1350	1376	C-H bending	alkanes
Less than 950	886,721, 619, 479	O-H bending	Alcohols, phenols, esters, ethers

alcohol and phenols. The hemicellulose, cellulose, and lignin O-H functional groups that are present in DBP bio-oil. In region B, two distinct peaks were detected at wavenumbers 2854 cm^{-1} and 2925 cm^{-1} within the range of 3000 cm^{-1} to 2800 cm^{-1}. These peaks are indicative of C-H stretching, specifically associated with the presence of alkanes. In region C, another two distinct peaks were detected at wavenumbers 1710 cm^{-1} and 1639 cm^{-1} within the range of 1620 cm^{-1} to 1850 cm^{-1}. The peaks indicate the presence of ketones, aldehydes, and carboxylic acids due to C=0 stretching. In region D, two notable peaks observed at wavenumbers 1376 cm^{-1} and 1455 cm^{-1}. These peaks correspond to C-H bending and C=C stretching, respectively. The presence of the peak at 1376 cm^{-1} suggests the presence of alkanes, while the peak at 1455 cm-1 indicates the presence of aroma

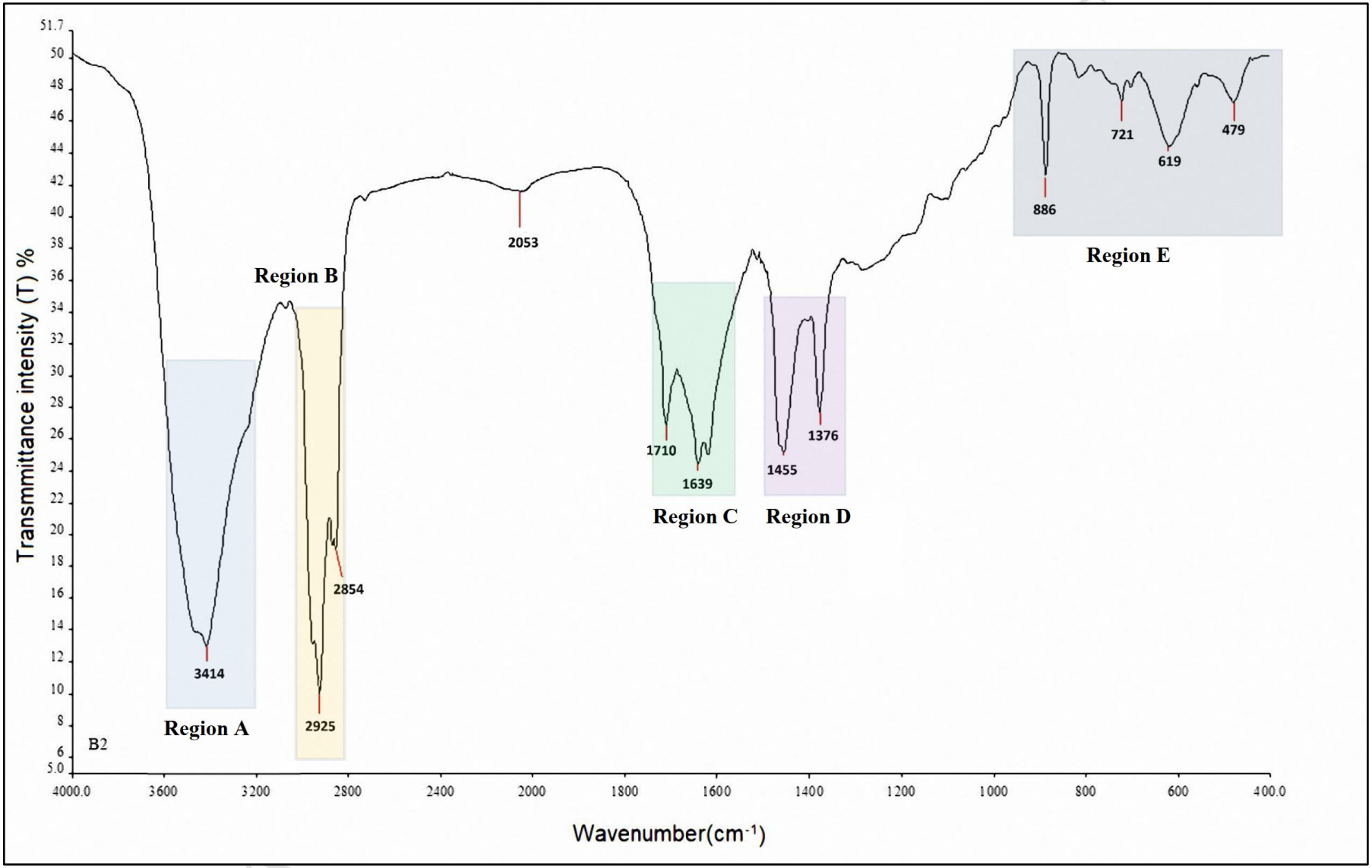

Figure 10: FTIR spectrum of bio-oil from optimization method.

aromatic compounds. The peaks at 886 cm^{-1}, 721 cm^{-1}, 619 cm^{-1}, 479 cm^{-1} are assigned to O-H bending indicates the presence of Alcohols, phenols, esters, and ethers. For the FTIR analysis of BDP bio-oil, a wide peak between 3600 cm^{-1} and 3200 cm^{-1} identified at 3414 cm^{-1} indicates the presence of phenols and alcohol. In addition, prominent peaks in the range of 3000 cm^{-1} to 2800 cm^{-1} at wavenumbers 2854 cm^{-1} and 2925 cm^{-1} indicate the presence of alkanes. The bio-oil also displays peaks at wavenumbers 1710 cm^{-1} and 1639 cm^{-1}, which are suggestive of C=0 stretching and connected to ketones, aldehydes, and carboxylic acids. Peaks at 1376 cm^{-1} and 1455 cm^{-1}, which are associated with C-H bending and C=C stretching, respectively, indicate the presence of alkanes and aromatic chemicals. O-H bending is also significant for the absorptions at 886 cm^{-1}, 721 cm^{-1}, 619 cm^{-1}, and 479 cm-^{1}, which denote the presence of phenols, alcohols, ethers, and esters. The analysis of DBP bio-oil revealed a large peak at wavenumber 3329.30 cm^{-1}, corresponding to O-H stretching, which is a kind of alcohols. Wavenumber 1631.50 cm^{-1} has a clear peak that is associated with the group of ketones' C=H bending. Another significant peak may be found at wavenumber 1400.70 cm^{-1}, which indicates N-H bending and secondary amines. In addition, the wavenumbers 1272.98 cm^{-1} and 1017.62 cm^{-1} show two separate peaks that belong to the ether group. Primary, secondary, and tertiary phenols, as well as other functional groups, are clearly present in BPS bio-oil. The O-H functional group bonds of the hemicellulose, cellulose, and lignin included in the BPS feedstock are represented by the absorptions at 3410 cm^{-1}, 3425 cm^{-1}, and 3736 cm^{-1}. The C-H stretching vibrations in the hemicellulose composition are responsible for the peaks at 2861 cm^{-1} and 2925 cm^{-1}. Additionally, the aromatic is related with absorbance peaks between 1400 cm^{-1} and 1600 cm^{-1} exhibiting C-C stretching. O-H bending is accountable for the peak that is lower than 1050 cm^{-1}. Overall, the distinctive spectrum characteristics and functional groups found in each sample of bio-oil show the variety of chemical compositions and possible uses of bio-oil obtained from various banana plant materials. These results offer important new information about how to characterise and use banana biomass for clean energy production and other industrial uses.

4.0. Future Recommendations

While the research objectives were met, there are several limits and openings for additional investigation that might increase its overall worth. To begin, a multi-stage condensing system, which was effectively applied in a previous study (Sadegh Papari, 2018), can be used to improve the condensation system of the pyrolysis process. To get different parts of the bio-oil, the system employs more condensers at variable temperatures and pressures. By improving the efficiency and recovery rate of the bio-oil, the quality of the final product can be improved while mitigating the environmental impact of the pyrolysis process. Secondly, a study on the optimization parameters of the pyrolysis process for bio-oil generation using banana peel can be conducted. The study will investigate how reactor operation is affected by temperature, heating rate, and nitrogen gas flow. By determining the optimal parameters for the pyrolysis process, the yield of bio-oil from banana peel can be maximized. Thirdly, further analytical tests may be used to find out more about the chemical composition of the bio-oil pyrolyzed from banana peel feedstock. These include gas chromatography (GC), nuclear magnetic resonance (NMR), and liquid chromatography (LC) for further examination of the bio-oil, as well as Gross Calorific Value (GCV) to estimate ash composition and calorific value for the banana peel feedstock. Last but not least, a thorough and comprehensive study of the manufacturing, processing, and use of biochar is required. The pyrolysis-produced biochar has potential uses in a number of fields of study, including soil science, renewable energy, and the prevention of climate change. Consequently, it is essential to know the biochar production process and discover ways to use it entirely as a valuable resource.

5.0. Conclusions

Banana peel, a chosen food waste, was effectively converted into bio-oil via slow pyrolysis in a lab-scale fixed-bed pyrolysis reactor. The Pyrolysis process was carried out to study the properties of the bio-oil using the feedstock dried under the optimization drying process parameter. An optimization study was conducted on the drying process using RSM analysis in Design Expert

to understand the optimization parameters required for maximum moisture content removal from the banana peel. The results of the RSM optimization and ANOVA analysis indicate that the CCD model utilized was statistically significant. Furthermore, the response of the fan speed and flap open variables within the model is significant towards the moisture content, which was the chosen response variable in the model. Therefore, TGA analysis was performed to investigate the thermal degradation behaviour of the dried banana peel, revealing a high content of hemicellulose, cellulose, and lignin decomposition with at least 70% of the content, indicating high potential for bio-oil generation. The TGA characteristics of biochar were significantly similar from the ASTM standard and optimization approach. The yield of bio-oil extracted from the 80-gram banana peel feedstock during the pyrolysis process was 16.6% at a temperature of 300°C, a heating rate of 10°C/min, a residual time of 90 minutes, and a nitrogen gas flow rate of 0.5 L/min. The extracted bio-oil was then analysed for its properties using CHNS and FTIR analysis, showing that it contained 69.12% carbon, 7.83% hydrogen, 5.97% nitrogen, and 0.95% sulphur, and generated 25.43 MJ/kg of higher heating value. The FTIR spectrum revealed the presence of alcohol, alkane, phenol, and primary alcohol in the bio-oil. Moreover, the proximate and ultimate analysis as well as the FTIR analysis were successfully carried out. The study's main objective was to examine the characteristics of bio-oil pyrolyzed from banana peels, a selected food waste, using a fixed-bed pyrolysis reactor, and to analyze the bio-oil components and chemical composition using CHNS and FTIR methods. As a result, the pyrolysis method's effective extraction of bio-oil from banana peels emphasizes the great potential of food waste as a source of renewable energy. In addition to providing an alternate strategy for dealing with the problem of food waste, this method also helps reduce greenhouse gas emissions and mitigate climate change. it is essential that governments and authorities take steps to facilitate the use of biomass renewable energy technologies, in particular the pyrolysis process. In the direction of a circular economy, where trash is converted into useful resources to provide a more sustainable in the future, it is the conversion of food waste into bio-oil constitutes an important step forward.

6.0. Acknowledgements

The authors express their appreciation for the financial support provided by University of Wollongong Malaysia, Postgraduate & Research Centre (PGRC), based in Utropolis Glenmarie, Malaysia. A special thank you also goes to Malaysia's Universiti Tunku Abdul Rahman for their guidance and financial assistance in ensuring the success of this project.

References

Ali, B. F., Ibraheem, F. H., Jassim, A. M., & Jassim, H. M. (2020). The Proximate Analysis method for the Composition Determination of Different Coal Types. *Proceedings of the 6th International Engineering Conference "'Sustainable Technology and Development'", IEC 2020*, 91–96. https://doi.org/10.1109/IEC49899.2020.9122917

Arun, A., Velmurugan, & Kumar, P. T. (2018). Production of Bio-Oil from banana peduncle by thermal cracking process. *Bulletin of Pure & Applied Sciences- Geology*, *37f*(1), 88. https://doi.org/10.5958/2320-3234.2018.00007.0

Bashir, M. J. K., Aziz, H. A., Yusoff, M. S., Adlan, M. N. (2010) Application of response surface methodology (RSM) for optimization of ammoniacal nitrogen removal from semi-aerobic landfill leachate using ion exchange resin. Desalination, 254, 154-161.

Bharathi, S. D., & Jacob, S. (2023). Comprehensive Treatment Strategy for Banana Inflorescence Bract to Synthesize Biodiesel and Bioethanol Through Fungal Biorefinery. *Waste and Biomass Valorization*. https://doi.org/10.1007/s12649-023-02166-9

C136/C136M-14:, A. (2019). Standard test methods for sieve analysis of fne and coarse aggregates. *ASTM International, United States*.

Chua, H. S., Bashir, M. J. K., Tan, K. T., & Chua, H. S. (2019). A sustainable pyrolysis technology for the treatment of municipal solid waste in Malaysia. *AIP Conference Proceedings*, *2124*(1). https://doi.org/10.1063/1.5117076

Ivanova, N., Gugleva, V., Dobreva, M., Pehlivanov, I., Stefanov, S., & Andonova, V. (2016). Application of Central Composite Design with Design Expert v13 in Process Optimization. *Intech*, *i*(tourism), 13.

Kabenge, I., Omulo, G., Banadda, N., Seay, J., Zziwa, A., & Kiggundu, N. (2018). Characterization of Banana Peels Wastes as Potential Slow Pyrolysis Feedstock. *Journal of Sustainable Development*, *11*(2), 14. https://doi.org/10.5539/jsd.v11n2p14

Kumar, M., Shukla, S. K., Upadhyay, S. N., & Mishra, P. K. (2020). Analysis of thermal degradation of banana (Musa balbisiana) trunk biomass waste using iso-conversional models. *Bioresource Technology*, *310* (February), 123393. https://doi.org/10.1016/j.biortech.2020.123393

López, H. D., Ayala, N., & Malagón-Romero, D. (2021). Evaluation of the Production of Bio-Oil Obtained Through Pyrolysis of Banana Peel Waste. *Chemical Engineering Transactions*, *89*(November), 637–642. https://doi.org/10.3303/CET2189107

Omulo, G., Banadda, N., Kabenge, I., & Seay, J. (2019). Optimizing slow pyrolysis of banana peels wastes using response surface methodology. *Environmental Engineering Research*, *24*(2), 354–361. https://doi.org/10.4491/EER.2018.269

Onsang, N., El Pebrian, D., & Anggraini, F. (2023). Sustainability of Malaysian smallholder banana farming: an energy efficiency use-based audit. *Agricultural Engineering International: CIGR Journal*, *25*(1), 111–122.

Pravin Kumar, S. A., Nagarajan, R., Midhun Prasad, K., Anand, B., & Murugavelh, S. (2022). Thermogravimetric study and kinetics of banana peel pyrolysis: a comparison of 'model-free' methods. *Biofuels*, *13*(2), 129–138. https://doi.org/10.1080/17597269.2019.1647375

Shehzad, A., Bashir, MJK., Sethupathi, S., Lim, JW., Younas M.(2016) Bioelectrochemical system for landfill leachate treatment–challenges, opportunities, and recommendations. Geosystem Engineering 19 (6), 337-345

Selvarajoo, A., & Hanson, S. (2014). Pyrolysis of Pineapple Peel: Effect of Temperature, Heating Rate and Residence Time on the Bio-char Yield. *Proceedings of the 2nd International Conference on Advances in Applied Science and Environmental Engineering - ASEE 2014*, *2*(1), 24–28.

Soetardji, J. P., Widjaja, C., Djojorahardjo, Y., Soetaredjo, F. E., & Ismadji, S. (2014). Bio-oil from Jackfruit Peel Waste. *Procedia Chemistry*, *9*, 158–164. https://doi.org/10.1016/j.proche.2014.05.019

Taib, R. M., Abdullah, N., & Aziz, N. S. M. (2021). Bio-oil derived from banana pseudo-stem via fast pyrolysis process. *Biomass and Bioenergy*, *148*(July 2020), 106034. https://doi.org/10.1016/j.biombioe.2021.106034

Yong, Z. J., Bashir, M. J. K., Ng, C. A., Sethupathi, S., Lim, J. W., & Show, P. L. (2019). sustainable Waste-to-Energy Development in Malaysia: Appraisal of Environmental , Financial , and Municipal Solid Waste. *Processes*, *7*(676), 29. www.mdpi.com/journal/processes

Yong, Z. J., Bashir, M. J. K., Hassan. MS. (2020)Assessment of environmental, energy and economic prospective of anaerobic digestion of organic municipal solid waste in Malaysia.

IOP Conference Series: Earth and Environmental Science 463 (1), 012054. **DOI** 10.1088/1755-1315/463/1/012054